Journal of Solid State Chemistry **164,** 12–18 (2002)
doi:10.1006/jssc.2001.9420, available online at http://www.idealibrary.com on IDEAL®

Synthesis, Crystal Structure, and Magnetic Properties of the Linear-Chain Cobalt Oxide $Sr_5Pb_3CoO_{12}$

K. Yamaura,*,†,[1] Q. Huang,‡,§ and E. Takayama-Muromachi*

*Advanced Materials Laboratory, National Institute for Materials Science, 1-1 Namiki, Tsukuba, Ibaraka 305-0044, Japan; †Japan Science and Technology Corporation, Kawaguchi, Saitama 332-0012, Japan; ‡NIST Center for Neutron Research, National Institute of Standards and Technology, Gaithersburg, Maryland 20899; and §Department of Materials and Nuclear Engineering, University of Maryland, College Park, Maryland 20742

Received January 5, 2001; in revised form October 2, 2001; accepted October 5, 2001

The novel spin-chain cobalt oxide $Sr_5Pb_3CoO_{12}$ [$P\bar{6}2m$, $a = 10.1093(2)$ Å and $c = 3.562\ 51(9)$ Å at 295 K] is reported. A polycrystalline sample of the compound was studied by neutron diffraction (at 6 and 295 K) and magnetic susceptibility measurements (5 to 390 K). The cobalt oxide was found to be analogous to the copper oxide $Sr_5Pb_3CuO_{12}$, which is comprised of magnetic-linear chains at an interchain distance of 10 Å. Although the cobalt oxide chains (μ_{eff} of 3.64 μ_B per Co) are substantially antiferromagnetic ($\theta_W = -38.8$ K), neither low-dimensional magnetism nor long-range ordering has been found; a local-structure disorder in the chains might have an impact on the magnetism. This compound is highly electrically insulating.

I. INTRODUCTION

In order to reveal the nature of correlated electrons in condensed matter and to construct advanced models for those, a one-dimensional (1D) electronic system as a basis of the models has been subjected to both experimental and theoretical investigations. In the experimental part, a variety of quantum phenomena have been found for the quasi-1D compounds in the past few decades: Tomonaga–Luttinger-type electric conductivity for $BaVS_3$ (1), Peierls instability for $CuGeO_3$ (2), charge- and spin-density waves for $(TMTSF)_2AsF_6$ and TTF-TCNQ (3, 4), spinon–holon separation for $SrCuO_2$ (5), Haldane gap for $Ni(C_2H_8N_2)_2NO_2(ClO_4)$ (6), and superconductivity for $(TMTSF)_2PF_6$ (7). These characteristic phenomena might reflect the nature of the correlated electrons, and intensive research on the materials played on important role in steadily advancing our understanding of their nature. We have recently been exploring novel quasi-1D compounds in order to find additional systems showing correlations among their magnetic and electronic transport properties, and crystal structure.

The linear-chain cobalt oxide $Sr_5Pb_3CoO_{12}$ was recently discovered in the course of studies of quasi-1D magnetic materials and their electrical-carrier-doped analogues (8–12). The polycrystalline sample of the compound was obtained by high-temperature solid-state reaction, and then subsequently investigated by X-ray diffraction, magnetic susceptibility, and thermogravimetric analysis (TGA) studies. The crystal structure was investigated in detail by powder-neutron diffraction at 6 and 295 K. The compound was found to be isostructural with the 1D antiferromagnetic copper oxide $Sr_5Pb_3CuO_{12}$ [$P\bar{6}2m$, $a = 10.1089(6)$ Å and $c = 3.5585(2)$ Å], in which distorted CuO_4 units are linearly connected by sharing those corner oxygens (8, 11, 12). The spin-singlet ground state, which potentially results from linear alternation of quantum spins, was suggested to have the composition $Sr_5Pb_{2.6}Bi_{0.4}CuO_{12}$ (8). Although the title antiferromagnetic compound $Sr_5Pb_3CoO_{12}$ was therefore expected to present one-dimensionally anisotropic magnetism, Curie–Weiss(CW)-type magnetism was eventually observed even at low temperature (>5 K). The rather isotropic magnetic property probably indicates a lack of 1D magnetic uniformity, which may be affected by a high degree of structural disorder in chains, as in the Bi-nondoped copper analogue (8). In this paper, the crystal structure and magnetic properties of the novel chain compound are reported and compared with those of the analogous copper oxides.

II. EXPERIMENTAL

The samples of the cobalt oxide were prepared as follows. A mixture of pure ($\geq 99.9\%$) and fine powders of $SrCO_3$, PbO, and Co_3O_4 (Sr:Pb:Co = 5:3:1 molar ratio, ~ 7 g) was placed in a dense-alumina crucible with a cap and heated in air at 750°C for 19 hours. The sample was quenched at room temperature and then ground. Thereafter, the

[1]To whom correspondence should be addressed. E-mail: YAMAURA.Kazunari@nims.go.jp. Fax.: + 81-298-58-5650.

0022-4596/02 $35.00

powder was reheated at 850, 900, and 950°C in turn for 66 hours in total. The preheated powder was then molded into several pellets, followed by heating at 970°C for 73 hours in air. Subsequently, some of the sintered pellets were annealed at 500°C in mixed gas, 20% oxygen in argon, at 100 MPa for 5 hours in a commercial apparatus (hot-isostatic-pressing system, developed by Kobe Steel, Ltd.). To qualitatively analyze the polycrystalline samples, X-ray diffraction at room temperature with Cu$K\alpha$ radiation was employed. The X-ray apparatus (RINT-2000 system, developed by Rigaku, Co.) was equipped with a graphite monochromator on the counter side and an autodivergence-slit system. The oxygen content of the samples was measured in a commercial TGA apparatus (PYRIS 1, developed by Perkin Elmer, Inc.) by heating a small amount of each sample (powder, $\sim$ 20 mg) in 3% hydrogen in argon at a heating rate of 5°C per minute to 700°C and holding for 6 hours.

To investigate the crystal structure further, the sample annealed in the compressed gas was again studied by neutron diffraction. The neutron data at 6 and 295 K were obtained by the BT-1 high-resolution powder diffractometer at the NIST Center for Neutron Research. A Cu(311) monochromator was employed to produce a coherent neutron beam ($\lambda = 1.5401$ Å) with 15′, 20′, and 7′ collimators before and after the monochromator, and after the sample, respectively. The neutron diffraction patterns were measured between 8 and 160° in diffraction angle at 0.05° per step. With the neutron profiles, crystal structure parameters were refined to a high degree of agreement by Rietveld calculations with the program GSAS (13). The total numbers of reflections and data points were 172 and 3039, respectively. Neutron scattering amplitudes in the calculations were set 0.702, 0.940, 0.253, and 0.581 ($\times 10^{-12}$) cm for Sr, Pb, Co, and O, respectively (13).

The magnetic properties of the samples were studied by using a commercial apparatus (MPMS system) between 5 and 390 K, developed by Quantum Design, Inc. The magnetic susceptibility data were collected at 50 kOe on cooling, and magnetization curves were recorded between -55 and 55 kOe after cooling of each sample at 5 and 150 K. All the pellets thus obtained were too electrically insulating to be subjected to further electronic transport measurements, beyond the 10 MΩ limit of a conventional two-terminal tester at room temperature.

III. RESULTS AND DISCUSSIONS

The power X-ray patterns of the annealed sample and the as-made sample are presented in Figs. 1a and 1b, respectively. Recalling the hexagonal unit cell of the structure of the analogous copper oxide $Sr_5Pb_3CuO_{12}$ [$P\bar{6}2m$, $a = 10.1089(6)$ Å and $c = 3.5585(2)$ Å] (8), a hexagonal unit cell was, at first, tested to qualitatively analyze the two patterns.

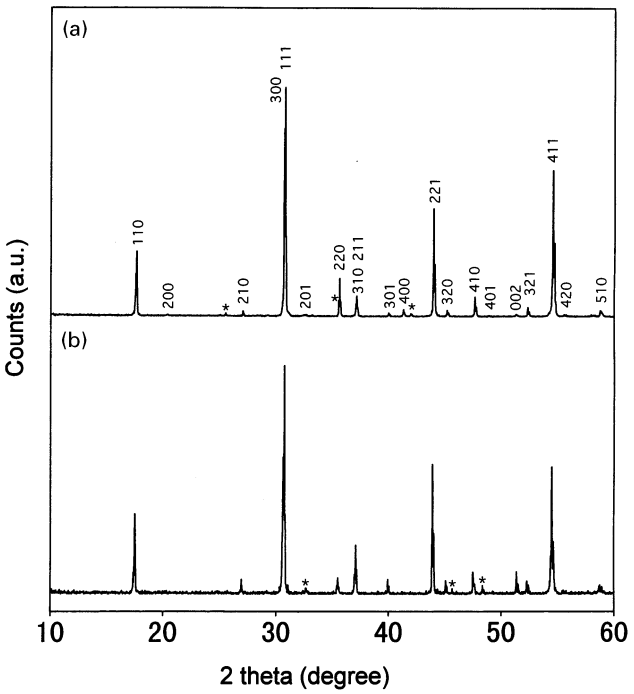

FIG. 1. Plots of X-ray profiles (Cu$K\alpha$) of powder samples of the cobalt oxide (a) annealed in the compressed oxygen–argon gas and (b) as-made in air. The data were obtained at room temperature. Small peaks marked by stars have not been indexed by the hexagonal-unit-cell model.

Peaks were clearly found to be at the expected positions from the hexogonal symmetry and lattice parameters, as marked by each *hkl* notation (Fig. 1a), except for several small peaks indicated by solid stars. The lattice parameters were refined to $a = 10.11(1)$ Å and $c = 3.567(1)$ Å by a least-squares fitting for the annealed sample pattern (Fig. 1a), and $a = 10.12(1)$ Å and $c = 3.558(1)$ Å for the other (Fig. 1b). The two patterns indicate the quality of the samples. Although the hexagonal model was eventually found reasonable to explain the X-ray peaks for the both cobalt oxides and the copper oxide, the star-marked minor peaks, however, remained to be uncharacterized, indicating the possible presence of either a small amount of impurities or somewhat of a structural modulation. An attempt to prepare a very pure sample, which may not show the extra peaks, by means of optimizing the heating conditions and starting compositions has been made; however, it has been unsuccessful thus far.

In order to measure the oxygen content of the cobalt oxide, a TGA study was made on selected samples; the data are shown in Fig. 2, where dotted and solid curves indicate weight change for the as-made and annealed samples, respectively. A clear weight loss was found above approximately 400°C in both measurements. Based on the hypothesis that the observed weight loss is totally due to oxygen reduction, the oxygen quantity was then calculated to be 12.19 and 12.32 moles per formula unit for the as-made and

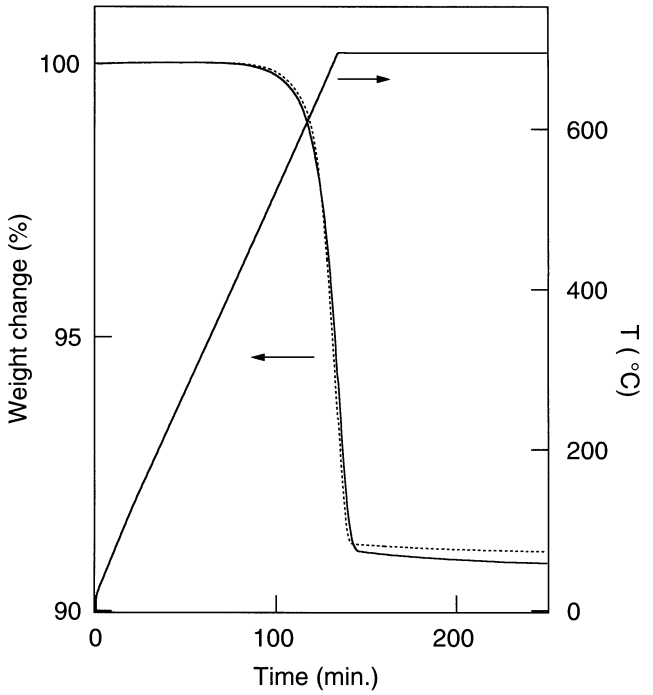

FIG. 2. Thermogravimetric analysis data for the powder samples as-made (dotted curve) and annealed in the compressed oxygen–argon gas (solid curve). The samples have been studied in a mixed gas, 3% hydrogen in argon, at a heating ratio of 5°C per minute. The weight losses at the major steps were 8.903% (solid curve) and 8.758% (broken curve), which suggest oxygen quantities in the samples of 12.32 and 12.19 moles per formula unit, respectively.

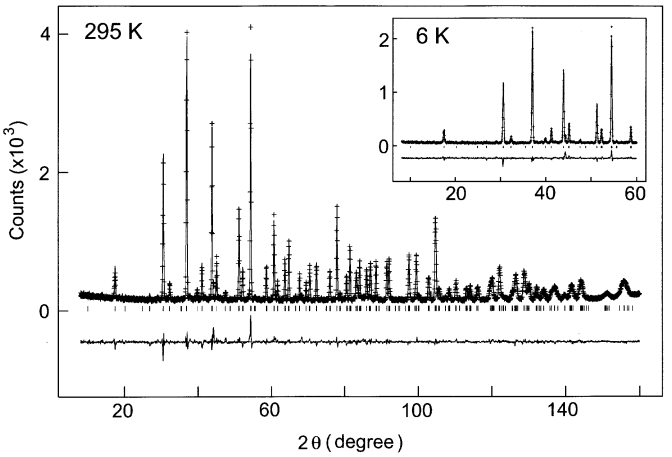

FIG. 3. Plots of the observed (crosses) and calculated (solid curve) neutron diffraction profiles (295 K, $\lambda = 1.5401$ Å) of the powder sample of $Sr_5Pb_3CoO_{12}$, annealed in the compressed gas. The vertical bars indicate calculated positions for the nuclear Bragg reflections. The lower part shows the difference between the profiles. The data of 6 K and the subsequent analysis of those are presented in the inset.

annealed samples, respectively. The high-oxygen-pressure annealing does not appear to produce a significant increment of oxygen quantity of the cobalt oxide. This fact is supported by the X-ray data; rather small changes (less than 0.25%) in lattice parameters were found after the annealing. As the samples continue to lose weight after the oxygen reduction is completed (null data secured the accuracy of the measurements), probably due to volatility of lead, a small amount of extra loosing should be superimposed on the major steps, which lead to some overestimation in the oxygen-quantity calculations.

The annealed sample was subjected to a neutron diffraction study at 6 and 295 K to obtain details of the local-chain structure and the degree of oxygen nonstoichiometry. The analysis of the neutron data using the Rietveld technique fundamentally followed the method developed for the structural studies on the analogous copper oxide $Sr_5Pb_3CuO_{12}$ (8, 11, 12). As a result, good results were obtained by the Rietveld calculations on the neutron profiles (Fig. 3), suggesting that the average crystal structural model ($P\bar{6}2m$) is reasonable with the cobalt oxide as well as the copper oxide (8, 11, 12). In the main panel of Fig. 3, the observed and calculated profiles are presented at the best quality (5–7% agreement factors). Shown below the profiles as a difference plot between those, the quality of the refinement is indeed convincing. The structure parameters of the best quality are listed in Table 1, and selected interatomic distances and bond angles were calculated from the parameters as in

TABLE 1
Structure Parameters of $Sr_5Pb_3CoO_{12}$ at 295 K (First Line) and 6 K (Second Line)[a]

Atom	Site	x	y	z	n	B (Å^2)
Sr(1)	2*d*	$\frac{1}{3}$	$\frac{2}{3}$	$\frac{1}{2}$	1	1.302(86)
		$\frac{1}{3}$	$\frac{2}{3}$	$\frac{1}{2}$	1	0.617(81)
Sr(2)	3*g*	0.70079(25)	0	$\frac{1}{2}$	1	0.829(51)
		0.70126(27)	0	$\frac{1}{2}$	1	0.519(52)
Pb	3*f*	0.33842(19)	0	0	1	0.897(29)
		0.33827(20)	0	0	1	0.545(31)
Co	2*e*	0	0	0.366(7)	0.5	3.80(56)
		0	0	0.349(8)	0.5	3.17(53)
O(1)	3*g*	0.1764(5)	0	1/2	0.795(23)	2.94(25)
		0.1779(6)	0	$\frac{1}{2}$	$= n$(295 K)	2.47(13)
O(2)	3*g*	0.46117(35)	0	$\frac{1}{2}$	1	1.320(65)
		0.4617(4)	0	$\frac{1}{2}$	1	0.765(62)
O(3)	6*j*	0.23757(22)	0.4418(4)	0	1	0.943(41)
		0.23797(24)	0.4428(4)	0	1	0.662(43)
O(4)	6*i*	0.1419(30)	0	0.271(8)	0.086(5)	2
		0.1499(31)	0	0.282(7)	$= n$(295 K)	1.2
O(5)	6*i*	0.9746(28)	0	0.896(5)	$= n$[O(4)]	2
		0.9696(24)	0	0.896(5)	$= n$(295 K)	1.2
	$R_p =$	5.12%	$R_{wp} =$	6.66%	$\chi^2 =$	1.970
		6.79%		8.60%		1.428

[a]Space group: $P\bar{6}2m$. The lattice parameters are $a = 10.1093(2)$ Å, $c = 3.56251(9)$ Å at 295 K, and $a = 10.0877(2)$ Å, $c = 3.55587(9)$ Å at 6 K. The volume of the hexagonal unit cell is 315.31(2) Å^3 at 295 K and 313.38(2) Å^3 at 6 K. The calculated density is 6.89 g/cm^3 at 295 K and 6.93 g/cm^3 at 6 K.

TABLE 2
Selected Interatomic Distances and Angles of $Sr_5Pb_3CoO_{12}$ at 295 K (First Line) and 6 K (Second Line)

Atoms		Distances (Å)	Atoms		Distances (Å)
Sr(1)–O(2)	× 3	2.9446(5)	Pb–O(3)	× 2	2.0857(19)
		2.9376(5)			2.0841(21)
Sr(1)–O(3)	× 6	2.6600(24)	Pb–O(4)	× 2	2.209(29)
		2.6483(25)			2.149(30)
Sr(2)–O(1)	× 2	2.6335(21)		× 2	3.270(31)
		2.6257(23)			3.291(11)
Sr(2)–O(2)	× 1	2.422(4)	Pb–O(5)	× 4	3.321(13)
		2.417(5)			3.291(11)
Sr(2)–O(3)	× 4	2.5571(25)	Co–O(1)	× 3	1.847(9)
		2.5574(27)			1.873(10)
Sr(2)–O(4)	× 4	2.745(9)	Co–O(4)	[× 3	1.474(30)]
		2.722(8)		[	1.531(31)]
Sr(2)–O(5)	× 2	3.106(26)		× 3	1.932(32)
		3.052(23)			2.001(34)
	× 2	3.461(16)		× 3	2.68(4)
		3.476(15)			2.71(4)
Pb–O(1)	× 2	2.420(4)	Co–O(5)	[× 3	1.694(33)]
		2.404(4)		[	1.640(35)]
Pb–O(2)	× 2	2.1709(21)		× 3	1.905(33)
		2.1704(22)			1.968(35)
				× 3	2.645(30)
					2.701(32)

Atoms	Angles (°)	Atoms	Angles (°)
O(1)–Co–O(1)	113.5(6)	O(4)–Co–O(5)	44.5(11)
	112.2(7)		45.1(11)
O(1)–Co–O(4)	21.96(2)	O(4)–Co–O(5)	55.3(21)
	121.18(32)		58.1(14)
O(1)–Co–O(5)	71.2(8)	O(4)–Co–O(5)	121.0(10)
	69.1(8)		124.9(11)
O(1)–Co–O(5)	82.7(12)	O(4)–Co–O(5)	147.5(21)
	82.3(12)		150.2(21)
O(1)–Co–O(5)	100.7(10)	Co–O(5)–Co	155.9(26)
	101.0(9)		149.9(23)
O(1)–Co–O(5)	120.4(20)	Co–O(5)–Co	163.6(18)
	126.0(20)		160.3(15)

Table 2. Lattice constants at 295 K of the hexagonal unit cell are $a = 10.1093(2)$ Å and $c = 3.56251(9)$ Å, which essentially match the X-ray parameters.

During the refinements, temporary fits using unfixed isotropic atomic displacement parameters and occupancy factors for O(4) and O(5) had given only unreliable results, probably due to too low levels of those occupancy factors, less than 0.1. The situation was not improved even for the low-temperature data. The isotropic atomic displacement parameters at the oxygen sites O(4) and O(5) were, therefore, fixed at a conceivable level, 2.0 $Å^2$ (1.2 $Å^2$ at 6 K); calculations thereafter appeared to improve the situation. For the same reasons, the occupancy factor of O(5) was constrained to be equal to that of O(4). The occupancy factors of O(2) and O(3), the normally occupied sites, were fixed to be fully occupied in the final calculation because oxygen vacancy was found within one standard deviation of 1.00. The possible mixing between Sr and Pb was tested in a preliminary manner; however, no substantial degree of mixing was detected. The displacement parameter of Co is unusually large, probably reflecting the local structure disorder as in the copper oxide (8, 11, 12). The occupancy factors in the partially occupied sites, O(1), O(4), and O(5), are slightly higher than the expected values $\frac{2}{3}$, $\frac{1}{12}$, and $\frac{1}{12}$, respectively, from the oxygen stoichiometric composition of 12 moles per the formula unit. The oxygen quantity calculated from the present neutron parameters is 12.42 moles per for formula unit. Although the estimation from the neutron data matches that of the TGA data (12.32 moles) within 1%, we believe the oxygen quantity may be slightly overestimated because the occupancy factors of O(4) and O(5) are too low to be accurate. As the neutron diffraction study on the copper oxide did not help to figure out the probable local-structure disorders and oxygen nonstoichiometry (8, 11, 12), further evaluation of the present analysis, including calculations

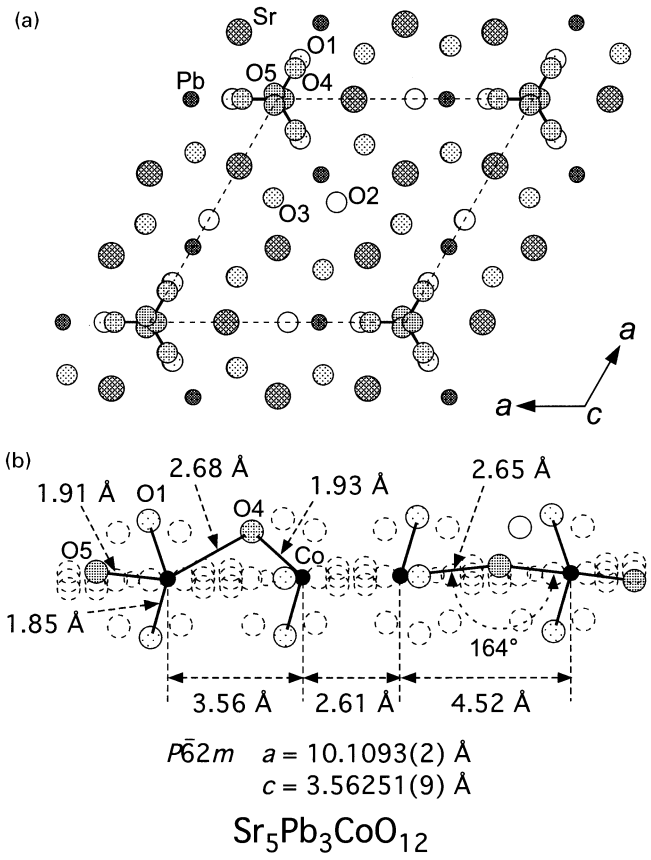

FIG. 4. (a) Schematic crystal structure view of $Sr_5Pb_3CoO_{12}$ drawn from the 295 K, neutron data. The hexagonal unit cell is indicated by the broken lines. (b) Schematic view of the cobalt–oxygen chain along the *c*-axis, showing the randomly occupied oxygen positions [O(1), O(4), and O(5)], and a probable arrangement of cobalt and oxygen atoms within the average structural model.

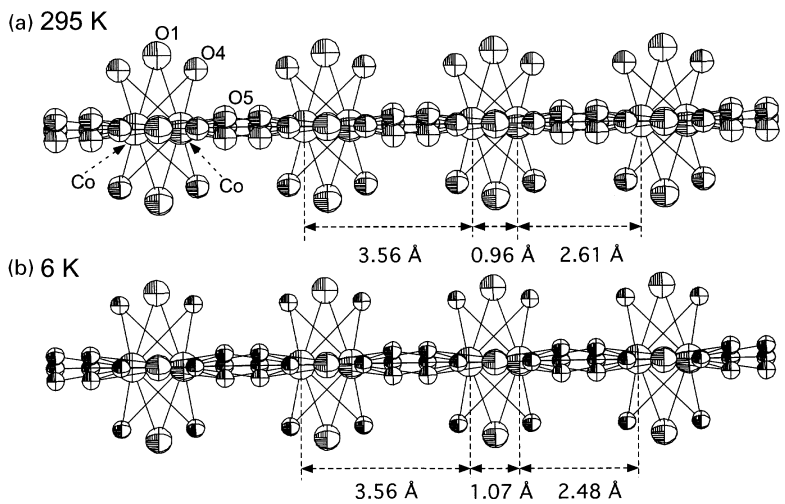

FIG. 5. Comparison of the chain structures at (a) 295 K and (b) 6 K of $Sr_5Pb_3CoO_{12}$ along the *c*-axis. The isotropic atomic displacements are shown.

with anisotropically thermal parameters of metals, did not shed light on the problem, either. The oxygen composition of the cobalt oxide might be slightly superstoichiometric ($\lesssim 12.4$), but not far from the stoichiometric $Sr_5Pb_3CoO_{12}$. To determine the oxygen quantity conclusively, further investigations would be required after very high-purity sample becomes available.

Schematic structural views of $Sr_5Pb_3CoO_{12}$ were drawn from the neutron data (295 K) in Figs. 4a and 4b. It is clear that the cobalt compound has a linear-chain structure basis, in which cobalt–oxygen polyhedra form chains at an interchain distance of 10.1 Å (8). A part of the chain along the *c*-axis is presented in Fig. 4b. All of the cobalt and oxygen sites are shown by the smaller and larger dotted circles, respectively, and the probable arrangement of those atoms is indicated by solid and filled circles. Intolerably short bond distances (Table 2) between cobalt and oxygen atoms were precluded from making the arrangement. The irregular arrangement of cobalt atoms, as shown in Fig. 4b, and the probable presence of local displacements of atoms may account for the observed unusually large atomic displacement parameters in the average-structure data such as 3.8 $Å^2$ and 2.9 $Å^2$ for Co and O(1), respectively. The *c*-axis constant (3.56251(9) Å) reflects the average of Co-to-Co distances in the chains; most are close to ~ 3.56 Å, but a few at ~ 2.61 Å may also be involved. Since the oxygen-coordination environment of all cobalt atoms is not unique, the degree of magnetic uniformity of the present chain compound might be as low as that of the copper oxide $Sr_5Pb_3CuO_{12}$, contrasted to other well-studied spin-chain compounds (14–17).

The low-temperature structure was investigated at 6 K (inset of Fig. 3) in the same manner, and the obtained structure parameters, calculated interatomic distances, and bond angles are summarized in Tables 1 and 2 as well. The hexagonal unit cell shrinks slightly (0.21% along the *a*-axis and 0.17% along the *c*-axis) upon cooling, while the Co site-splitting is more conspicuous than that at 295 K (+ 11.5% in splitting distance) as shown in Figs 5a and 5b. No traces of magnetic ordering were detected in the diffraction profiles.

The magnetic susceptibility data of the samples annealed (open circles) and as-made (closed circles) are shown in Fig. 6; T vs $1/\chi$ and T vs χ are plotted in the main panel and the inset, respectively. The data of magnetic field dependence of the magnetization at 5 and 150 K are shown in Fig. 7. Seen in the main panel of Fig. 6, the inverse magnetic susceptibility is linearly dependent on temperature above approximately 130 K for both samples. The CW law was then applied to analyze the two sets of high-temperature data. The formula to fit the data by a least-squares method, as indicated by the solid lines (main panel of Fig. 6), was

$$\chi(T) = \frac{N\mu_{\text{eff}}^2}{3k_{\text{B}}(T - \theta_{\text{W}})} + \chi_0, \qquad [1]$$

where θ_{W}, χ_0, μ_{eff}, k_{B}, and N are Weiss temperature, temperature-independent term, effective magnetic moment, Boltzmann constant, and Avogadro's constant, respectively. In a preliminary fit, the temperature-independent term χ_0 was estimated to be on the order of 10^{-6} emu/mol-Co, which was negligibly small, and thus we decided not to employ the second term in Eq. [1] hereafter. The subsequent fits yielded μ_{eff} of 3.64 μ_{B} per Co and θ_{W} of -38.8 K for the annealed sample, and μ_{eff} of 3.83 μ_{B} per Co and θ_{W} of -44.5 K for the as-made sample; those parameters were characteristic of antiferromagnetic interaction. As the oxygen stoichiometry is vague (12 to 12.4 moles per formula unit), the

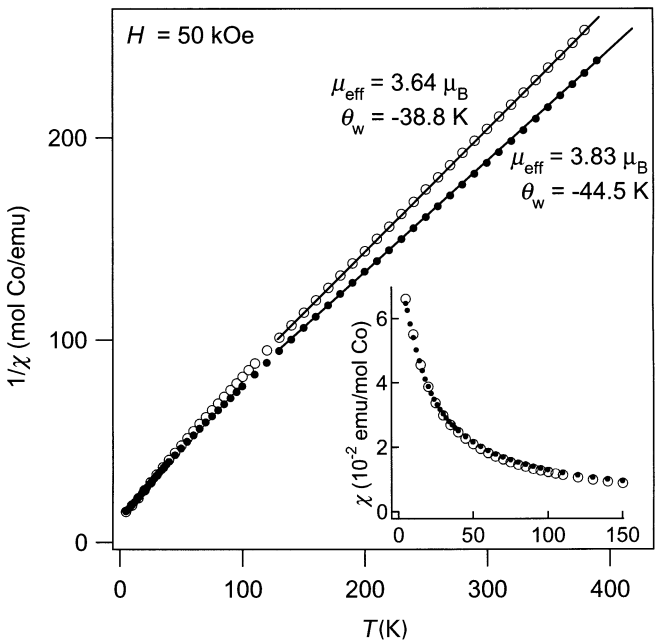

FIG. 6. Temperature dependence of the inverse magnetic susceptibility and the magnetic susceptibility at 50 kOe of the cobalt oxides as-made (closed circles) and annealed in the compressed oxygen–argon gas (open circles). The solid line indicates fits to the Curie–Weiss law.

formal valence of cobalt also becomes indefinite about $+2$ to $+2.8$ when the valence of lead is $+4$. Due to the rather large degree of uncertainty of the valence of cobalt at about 40%, it is impossible to determine the electronic configuration of cobalt solely from the magnetic susceptibility data. Further investigations, including spectroscopic studies, might help to clarify the issue.

Seen in Fig. 6, a characteristic maximum expected from 1D antiferromagnetism in T vs χ plot for either Bonner–Fisher or spin-gap models was not observed at all, although the chains were substantially antiferromagnetic (14–17). Below approximately 100 K, the inverse magnetic susceptibility gradually starts to diverge from the CW line to go down on cooling, indicative of gradual growth of a ferromagnetic component in short range. To study the low-temperature portion further, the Brillouin function was employed to make a comparison with the magnetization data at 5 K (Fig. 7). The function to calculate the ideal M_S vs H curve at 5 K for free spins (S) was

$$M_S(\alpha) = NgS\mu_B\left(\frac{2S+1}{2S}\coth\frac{2S+1}{2S}\alpha - \frac{1}{2S}\coth\frac{1}{2S}\alpha\right), \quad [2]$$

where $\alpha = gS\mu_B H/k_B T$. The effective S was estimated to be ~ 1.39 for the annealed and ~ 1.48 for the as-made samples from calculations using the formula $\mu_{\text{eff}} = 2\sqrt{S(S+1)}$ and the μ_{eff} parameters, obtained by the CW fits. The computed curves for free spins at the both S values are shown in Fig. 7. Due to the substantial antiferromagnetic interactions, the magnetization at 50 kOe for the cobalt oxides is reduced to approximately one-third of that for the ideal-free-spin system. Although the absolute Weiss temperatures are much higher than the studied temperature of 5 K, the magnetization depends on applied field with positive curvature rather than a linear relationship, which may indicate somewhat of an influence of the ferromagnetic spin coupling (Fig. 7). These observations, including the deviation from the CW line on cooling, suggest that minor ferromagnetic interactions coexist with the antiferromagnetism, and might help to destroy the potential 1D-antiferromagnetic character. Since the chain involves local-structure disorder and can potentially be modulated, the characters of all probable magnetic bonds were unable to be uniquely determined in this way. The observed θ_W, which is apparently negative, is probably due to a balance between the major antiferromagnetic and the possible minor ferromagnetic interactions. The observed ferromagnetic component, otherwise, results from minor magnetic impurities.

In summary, we have reported the average structure and the magnetic properties for the quasi-1D novel cobalt oxide. Due to the probable presence of local-structure disorders such as the local displacement of cobalt and ligand oxygens,

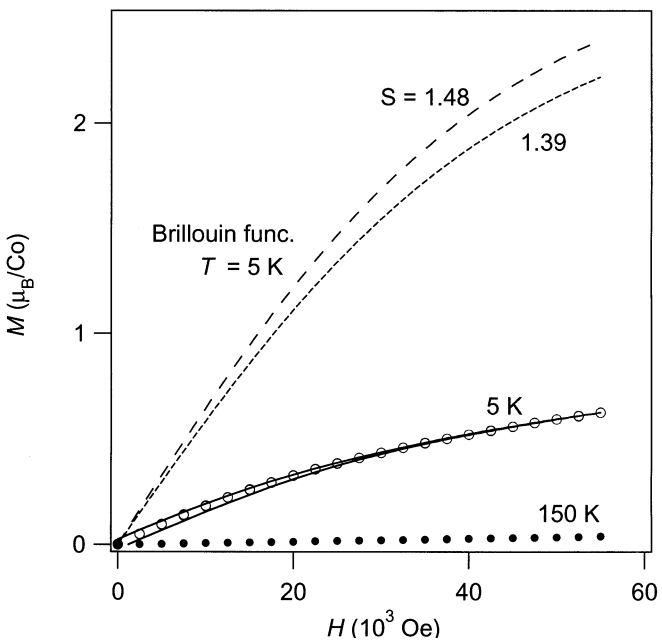

FIG. 7. Applied magnetic field dependence of the magnetization of the annealed sample of $Sr_5Pb_3CoO_{12}$ at 5 and 150 K. The solid curves are the data at 5 K obtained prior to the annealing. Estimated spin numbers ($S = 1.48$ and 1.39) by the Curie–Weiss fits to the high-temperature data were employed to compute the broken curves for free spins at 5 K using the Brillouin function.

and the irregular arrangement of cobalt–oxygen polyhedra in short range, the degree of magnetic coherence should not be as high as expected to the low-dimensional magnetism. The local structure is too complicated to be clearly observed by neutron diffraction which probes a positional average of the structure. Further studies with local structural and magnetic probes, which are more sensitive to the microscopic magnetic environment, could clarify the probable coupling between the local-structure disorders and the rather unusual magnetism.

ACKNOWLEDGMENTS

This research was supported in part by the Multi-Core Project administrated by the Ministry of Education, Culture, Sports, Science and Technology of Japan.

REFERENCES

1. M. Nakamura, A. Sekiyama, H. Namatame, A. Fujimori, H. Yoshihara, T. Ohtani, A. Misu, and M. Takano, *Phys. Rev. B* **49,** 16191 (1994).
2. M. Hase, I. Terasaki, and K. Uchinokura, *Phys. Rev. Lett.* **70,** 3651 (1993).
3. K. Mortensen, Y. Tomkiewicz, and K. Bechgaard, *Phys. Rev. B.* **25,** 3319 (1982).
4. S. Kagoshima, T. Ishiguro, and H. Anzai, *J. Phys. Soc. Jpn.* **41,** 2061 (1976).
5. C. Kim, A. Y. Matsuura, Z. X. Shen, N. Motoyama, H. Eisaki, S. Uchida, T. Tohyama, and S. Maekawa, *Phys. Rev. Lett.* **77,** 4054 (1996).
6. Y. Ajiro, T. Goto, H. Kikuchi, T. Sakakibara, and T. Inami, *Phys. Rev. Lett.* **63,** 1424 (1989).
7. D. Jerome, A. Mazaud, M. Ribault, and K. Bechgaard, *J. Phys. Lett.* **41,** L95 (1980).
8. K. Yamaura, Q. Huang, and E. Takayama-Muromachi, *Phys. Rev. B* **64,** 184428 (2001).
9. K. Yamaura and R. J. Cava, *Solid State Commun.* **115,** 301 (2000).
10. K. Yamaura, H. W. Zandbergen, K. Abe, and R. J. Cava, *J. Solid State Chem.* **146,** 96 (1999).
11. J. S. Kim, X. X. Tang, A. Manthiram, J. S. Swinnea, and H. Steinfink, *J. Solid State Chem.* **85,** 44 (1990).
12. T. G. N. Babu and C. Greaves, *J. Solid State Chem.* **95,** 417 (1991).
13. A. C. Larson and R. B. Von Dreele, Los Alamos National Laboratory Report No. LAUR086-748, LANL, Los Alamos, NM, 1990.
14. J. C. Bonner and M. E. Fisher, *Phys. Rev. A.* **135,** 640 (1964).
15. J. C. Bonner, S. A. Friedberg, H. Kobayashi, D. L. Meier, and H. W. J. Blöte, *Phys. Rev. B* **27,** 248 (1983).
16. D. C. Johnston, J. W. Johnson, D. P. Goshorn, and A. J. Jacobson, *Phys. Rev. B* **35,** 219 (1987).
17. T. Barnes and J. Riera, *Phys. Rev. B* **50,** 6817 (1994).